ELSEVIER

Chemical Engineering Journal 140 (2008) 439–447

Chemical Engineering Journal

www.elsevier.com/locate/cej

Comparison of hydrodynamic and mass transfer performances of an emulsion loop-venturi reactor in cocurrent downflow and upflow configurations

B. Gourich [a,*], Ch. Vial [b], M. Belhaj Soulami [c], A. Zoulalian [d], M. Ziyad [e]

[a] *Laboratoire de Génie des Procédés, Ecole Supérieure de Technologie de Casablanca, BP 8012, Oasis Casablanca, Morocco*
[b] *Laboratoire de Génie Chimique et Biochimique, Université Blaise Pascal, 24 avenue des Landais, BP 206, F-63174, Aubière Cedex, France*
[c] *Laboratoire de Génie des Procédés et Environnement, ENIM BP 753 Agdal Rabat, Morocco*
[d] *Laboratoire de Génie des Procédés, ESSTIB, Université Henri Poincaré, BP 239, 54506 Vandœuvre Cedex, France*
[e] *Département de Chimie, Faculté des Sciences, Université Mohammed V, avenue Ibn Battouta, BP 1014, Rabat, Morocco*

Received 4 September 2007; received in revised form 5 November 2007; accepted 12 November 2007

Abstract

Hydrodynamic parameters (gas-induced flow rate and gas hold-up) and mass transfer characteristics (k_La, k_L and a) have been investigated in a gas–liquid reactor denoted "Emulsair" in which the distributor is an emulsion-venturi and the gas phase is self-aspired by action of the kinetic energy of the liquid phase at the venturi throat. Two configurations, respectively cocurrent downflow and cocurrent upflow were compared. A chemical method involving the dispersion of a CO_2–air mixture in a monoethanolamine (MEA) aqueous solution was used to measure mass transfer parameters. Experimental results showed that only the homogeneous bubbling regime prevailed in the upward configuration, while an annular regime could also be observed for cocurrent downflow at low liquid flow rate. Gas-induced flow rate and gas hold-up were usually smaller for cocurrent upflow, both at constant liquid flow rate and specific power input. The same stood for mass transfer properties. Conversely, specific power requirements were lower at constant liquid flow rate and mass transfer characteristics were enhanced at constant gas-induced flow rate for cocurrent upflow. A comparison with other gas–liquid contacting devices showed that the Emulsair reactor is a versatile tool avoiding the presence of mechanically moving parts when high and quickly adaptable dissolved gas supply is required. The cocurrent upflow configuration can be preferred when high gas flow rates are desired because the evolutions of gas-induced flow rate and mass transfer characteristics exhibit a stronger dependence on specific power input in the homogeneous bubbling regime for this configuration.

Keywords: Aeration; Chemical absorption; Emulsion venturi; Hydrodynamics; Mass transfer

1. Introduction

In gas–liquid and gas–liquid–solid reactions, the overall production rate is often limited by interphase mass transfer. Relatively large interfacial areas are particularly desirable when absorption is accompanied by a rapid chemical or biochemical reaction. This is particularly true for absorption, such as the treatment of industrial gaseous waste including the absorption of CO_2, H_2S, SO_2, NO_x, or VOCs, but also for aerobic fermentation and biological wastewater treatments that require high and quickly adaptable oxygen supply for enhancing the growth of micro-organisms. Many multiphase contacting devices have been described [1]. These differ mainly by the way the dispersion is achieved, the range of the overall gas fraction in the reactor, the interfacial area between the phases and the power requirements for gas dispersion. Three types can be distinguished:

- mechanically stirred tanks in which the driving force of gas dispersion is the power supplied by impellers;
- gas-driven reactors in which dispersion is induced by the gas phase, such as bubble columns with a continuous liquid phase, or packed columns with a continuous gas phase;

* Corresponding author. Tel.: +212 22 23 15 60; fax: +212 22 25 22 45.
E-mail address: gourich@est-uh2c.ac.ma (B. Gourich).

1385-8947/$ – see front matter © 2007 Elsevier B.V. All rights reserved.
doi:10.1016/j.cej.2007.11.011

- liquid-driven reactors in which the kinetic energy of the liquid phase is responsible for gas dispersion.

Venturi devices constitute a special type of gas–liquid contactors that belong both to the second and the third class of gas–liquid reactors, as a function of the gas-to-liquid flow rate ratio (Q_G/Q_L). Their first advantage is that dispersion is achieved through the kinetic energy of the continuous phase that can be either the liquid (emulsion venturi: $Q_G/Q_L < 1$) or the gas (jet venturi: $Q_G/Q_L > 10$), which may result in either bubbly flows or sprays, respectively. Another advantage is that venturi devices can be used as gas distributors when the reaction is slow, but also as chemical reactors when the kinetics is fast. Additionally, liquid-driven venturis can be easily used as gas-inducing devices; this may reduce the cost of gas supply or constitute a simple and cheap way for recycling the gas phase when this is pure, which is generally the case, for example, for hydrogenations and oxidations. However, there is still a lack of experimental data and modeling procedures to account for the hydrodynamic and mass transfer characteristics of gas–liquid venturi devices, especially when the liquid is the continuous phase, whereas there is an abundant literature on conventional bubble columns, aerated stirred tanks and on the comparison of their respective performance [2]. In the literature, liquid-driven venturis were used first as gas distributors in gas–liquid and gas–liquid–solid reactors without mechanical agitation, such as upward and downward bubble columns with an imposed gas flow rate [3,4]. For gas-inducing systems, Cramers et al. [5], Cramers and Beenackers [6] investigated ejectors, which constitute a particular class of venturi devices in which there is no converging section. Similarly, Cramers et al. [7] studied a particular ejector geometry in which the divergent was replaced by a straight tube. Hydrodynamic and k_La data from an emulsion loop-venturi reactor equipped with a conventional venturi with a cocurrent downflow configuration were reported by Gourich et al. [8]. A comparison of this "Emulsair" reactor with other gas–liquid contacting devices was described by Gourich et al. [9] as a function of specific power input. This reactor was shown to be a versatile tool for biochemical and wastewater treatments for which operating conditions have to be modified quickly without the need for mechanically moving parts.

The aim of this work is therefore to compare the hydrodynamic and mass transfer characteristics of cocurrent downflow and cocurrent upflow configurations of the "Emulsair" reactor as a function of liquid flow rate and specific power input. This comparison will include gas-induced flow rate, gas-hold-up, k_La, but also k_L and a parameters. A comparison with the performances of other conventional gas–liquid contactors, such as bubble column reactors or aerated stirred tanks will also be provided.

2. Materials and methods

Experiments were carried out in an "Emulsair" reactor that consisted of a transparent cylindrical tank (30 cm diameter and 0.03 m^3 liquid volume) with a conical bottom topped by an emulsion-venturi made of plexiglas to allow visual observation of flow regimes. The venturi consisted of a convergent (0.096 m length, 20° angle), a throat (0.02 m length) and a divergent (0.225 m length, 5° angle). The divergent is prolonged by an immersed gas–liquid distributor placed in the center of the tank. The liquid phase was totally recirculated in a "liquid loop". The main components of this liquid recirculation loop included a valve for flow control, a calibrated flowmeter, a heat exchanger to maintain constant liquid temperature (20 ± 1 °C) and a recirculation pump. The liquid flow rate Q_L was varied between 3.33×10^{-4} and 27.8×10^{-4} $m^3\,s^{-1}$. The gas phase (CO_2 + air) was self-aspired into the venturi by action of the kinetic energy of the liquid recirculation at the throat through four symmetrically radial orifices (1 cm diameter). The gas flow rate Q_G was dispersed in the divergent (0.24 L volume) and measured using a volumetric flowmeter. The gas–liquid emulsion was formed through three series of eight orifices laid out regularly on the surface of the distributor. The cocurrent downflow configuration has already been described in detail [8,9]. In this case, the liquid phase was recirculated from the bottom of the reactor and both phases were completely separated in the tank, which allowed the total recirculation of the liquid phase without bubbles. In the cocurrent upflow configuration (Fig. 1), the liquid loop was more complex because the liquid phase was recovered by overflow, which required an additional gas–liquid separation step with a constant liquid level separator to avoid bubble recirculation. Consequently, the feed tank of the downward configuration was used as the gas–liquid separator, which required an additional feed system for the upward configuration (Fig. 1). In both configurations, all the experiments were carried out at atmospheric pressure.

Gas hold-up ε_G in both configurations was measured using the volume expansion method. This was shown to be nearly as effective as a more accurate dynamic tracer technique in the Emulsair reactor, even when liquid level fluctuations occurred at high liquid flow rate [8]. The mass transfer parameters k_La, k_L and a were measured using a chemical method based on CO_2 absorption from a CO_2–air mixture in an aqueous solution of monoethanolamine (MEA). The modeling assumptions can be summarized as follows:

- both phases are perfectly mixed;
- the reaction takes place only in the divergent of the venturi, the pipe downstream from the venturi (corresponding to the distributor) and the reaction tank (V_{L1}: volume of the active zone which is the same in case of upflow and downflow);
- the gas-side resistance to mass transfer is negligible;
- mass transfer may be described by the film-penetration model;
- Henry's law applies at the gas–liquid interface.

The first assumption is in agreement with those proposed in the literature for similar systems [10–13]. Although it is clear that hydrodynamics and mass transfer differ between the venturi, the distributor and the tank, local measurements cannot be carried out directly in the divergent and the distributor. Furthermore, the gas dispersion coupled to the high liquid recirculation rate favors mixing of both phases in the tank [8]. However, this has been checked using RTD measurements in the gas phase

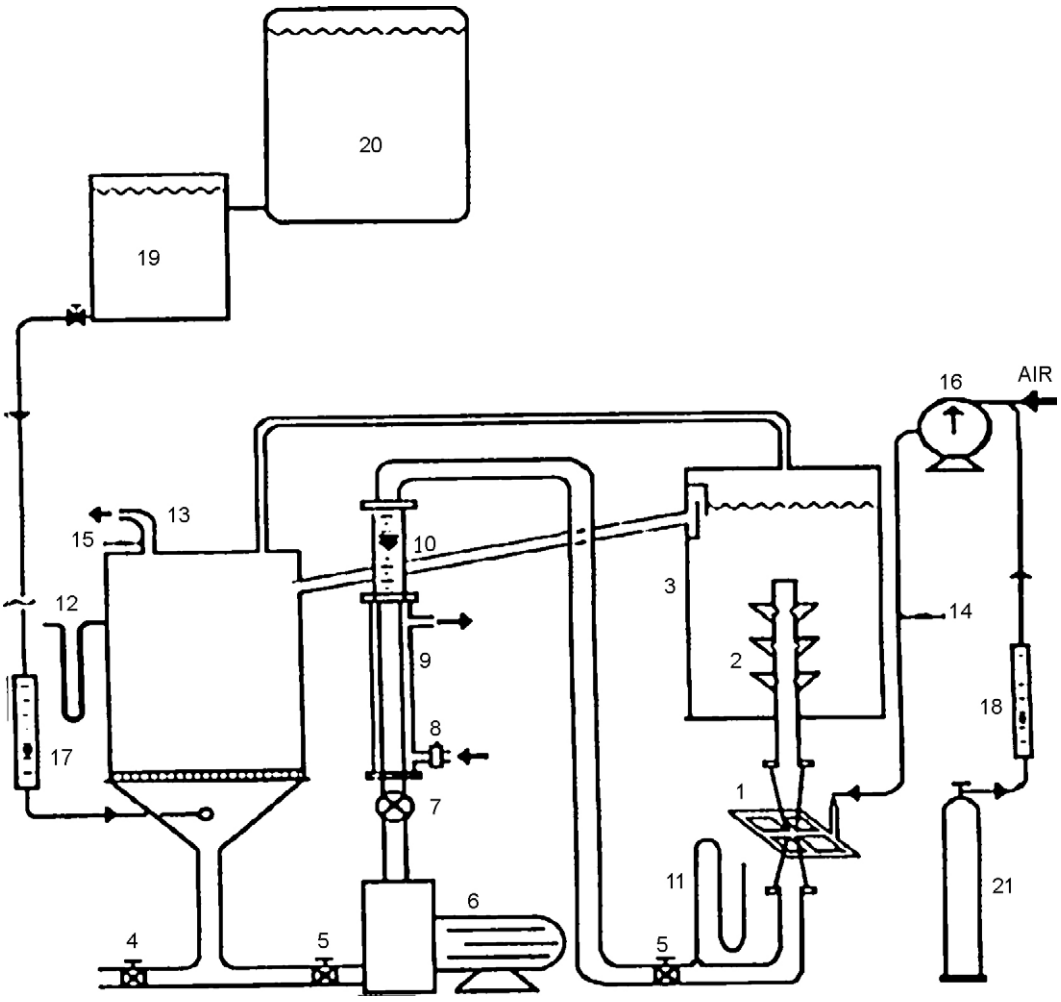

Fig. 1. Experimental set-up for the cocurrent upflow configuration: 1, emulsion venturi; 2, gas distributor; 3, reaction tank; 4, drain; 5, quarter-turn valve; 6, centrifugal pump; 7, liquid flow regulation valve; 8, electrovalve for temperature control; 9, heat exchanger; 10, liquid flowmeter; 11 and 12, overflow; 13, gas outlet; 14, gas sampling system (inlet) to TCD; 15, gas sampling system (outlet) to TCD; 16, gas volumetric flowmeter; 17, flowmeter; 18, CO_2 mass flow controller; 19 and 20, 40 L and 200 L feed tanks; 21, CO_2 bottle.

with helium as a low-solubility gas and we have also varied the inlet concentration of CO_2 over a wide range and shown that the estimates of k_L and a remain the same. These experiments have confirmed that the first zone is close to a perfectly mixed tank, although it includes the venturi and the distributor.

The overall volumetric mass transfer coefficient $k_L a$ was obtained when reaction rate was slow in the mass boundary layer around the bubbles, but rapid enough in the bulk so as to have no dissolved CO_2 in the liquid phase at the outlet of the reactor. This required that Hatta number (Ha) was lower than 0.3 (Eq. (1)).

$$Ha = \frac{\sqrt{D_{CO_2} k_2 [\mathrm{MEA}]}}{k_L} \quad (1)$$

Eq. (1) assumes a first-order reaction in CO_2 and MEA, in agreement with literature data [14]. k_2 the kinetic constant of the acid–base reaction, [MEA] the concentration of MEA in the reactor and $D_{CO_2} = 1.9 \times 10^{-9}\sqrt{1 - 4.11x}$ is the diffusion coefficient of CO_2 in the liquid phase that is a function MEA molar fraction x [15]. The Danckwerts plot technique was used to estimate simultaneously the mass transfer parameters, k_L and a, from mass transfer experiments when $0.3 < Ha < 3$. The mass transfer properties were obtained from a mass balance on the gas phase using gas chromatography (Porapak Q column) and a thermal conductivity detector (TCD) for the measurement of CO_2 concentration both in the inlet and the outlet gas streams of the reactor. Further details on the gas sampling system involving a pneumatically-controlled six-port valve are reported in Gourich et al. [8]. This method was faster than the direct measurements of MEA concentration in the liquid phase and allowed data acquisition using a RTI 815 A/D acquisition card; it gave directly access to the mass transfer rate Φ_{CO_2}. The prevailing absorption regime depended on the MEA concentration in the inlet stream that ranged between 0.02 and 2.0 mol/L, while CO_2 mole fraction in the inlet stream ranged between 1 and 5%. For $Ha^2 \ll 1$, $k_L a$ was directly estimated from Φ_{CO_2} and CO_2 solubility in the liquid phase $C^*_{CO_2,L}$ (Eq. (2)) that was obtained using Henry's constant $H_{CO_2} = 26.4\,\mathrm{bar\,m^3\,kg\,mol^{-1}}$ at 20 °C [15]:

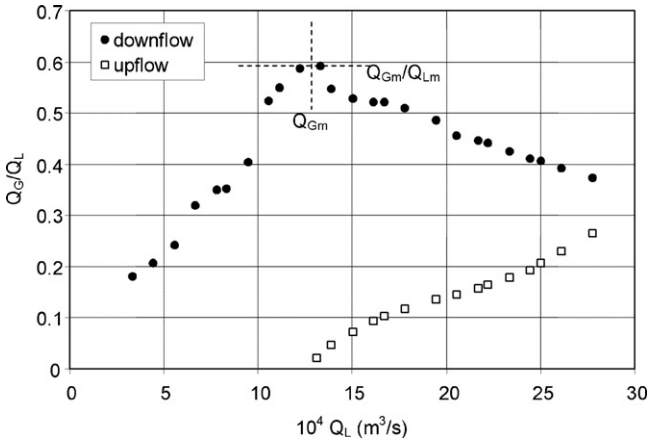

Fig. 2. Evolution of the Q_G/Q_L ratio as a function of Q_G.

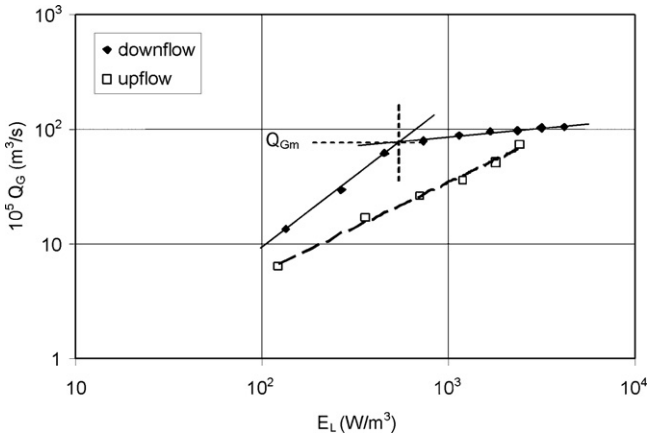

Fig. 3. Evolution of Q_G as a function of specific power input E_L.

$$\Phi_{CO_2} = k_L a V_{L1} C^*_{CO_2,L} \quad (2)$$

Ha calculation required the estimation of [MEA] that could be easily deduced from a mass balance on CO_2 on both phases. For k_L and a estimation, the Danckwerts method derived the following model when $0.3 < Ha < 3$:

$$\Phi_{CO_2} = a V_{L1} C^*_{CO_2,L} \sqrt{k_L^2 + D_{CO_2} k_2 [\text{MEA}]} \quad (3)$$

in which V_{L1} is the liquid volume of the reaction tank. This method consisted in plotting the $(\Phi_{CO_2}/C^*_{CO_2,L})^2$ ratio vs. [MEA]. The curve should be a straight line with $(aV_{L1}C^*_{CO_2,L})^2 D_{CO_2} k_2$ as the slope and $(k_L a V_{L1} C^*_{CO_2,L})^2$ as the intercept, which gave access to $k_L a$, a and consequently to k_L. Kinetic data (k_2) was measured in a falling film reactor in which the interfacial area and the mass transfer coefficient were known in advance. Experiments gave $k_2 = 4340\ m^3/kmol{\cdot}s$ at 20 °C and atmospheric pressure, which is in accordance with the literature [15]. The results obtained for $k_L a$ measurements for the downward configuration were in agreement with those obtained previously using the oxygenation dynamic method and a dynamic tracer technique [8]. For the emulsion loop reactors, the operating costs essentially depend on the kinetic energy of the liquid phase dissipated between the venturi throat and the liquid free surface in the reaction tank [16]. The specific power input for gas dispersion E_L (W/m³) was estimated from the Eq. (4) by measuring the pressure at the upstream of the venturi using bourdon manometer and the relative pressure at the throat (P_C). E_L can be deduced from the Bernoulli balance

$$E_L = \left(P_C + \frac{1}{2}\rho_L U_C^2 + \rho_L g \Delta z \right) \frac{Q_L}{V_{L1}} \quad (4)$$

in which U_C is the liquid velocity at the venturi throat (deduced from Q_L), ρ_L the liquid density and Δz the algebraic distance between the venturi throat and the liquid free surface in the reaction tank. The sign of the gravitational potential energy in Eq. (4) depended on the configuration: Δz was negative for cocurrent upflow and positive for cocurrent downflow.

3. Results and discussion

3.1. Hydrodynamics

For the emulsion loop-venturi reactors, a certain minimum liquid velocity at the venturi throat is needed for gas induction to start. In this case, according to the Bernoulli's principle, when the liquid is pumped at a high velocity, a low pressure is created in the throat of the venturi. The analysis of gas-induced flow rate Q_G showed that self-aspiration started when Q_L was higher than 2.78×10^{-4} and 13.1×10^{-4} m³/s for cocurrent downflow and cocurrent upflow configurations, respectively (Fig. 2). In both cases, Q_G was always an increasing function of Q_L, even when Q_G/Q_L decreased in the downward configuration at higher liquid flow rate. However, a crossover point could probably exist between the two Q_G/Q_L curves at higher liquid flow rate. As a result, gas-induced flow rates remained in the following ranges in this work, respectively $6.0 \times 10^{-5} \le Q_G \le 10.39 \times 10^{-4}$ m³/s and $2.89 \times 10^{-5} \le Q_G \le 7.40 \times 10^{-4}$ m³/s for downward and upward configurations. Actually, gas-induction started approximately at the same specific power input, about 100 W/m³, as shown by Fig. 3, which means that E_L was lower for cocurrent upflow at constant liquid flow rate. This is confirmed by Fig. 4 that plots the evolution of E_L vs. Q_L for both configurations. This behavior was indeed a direct consequence of Eq. (4). The lower

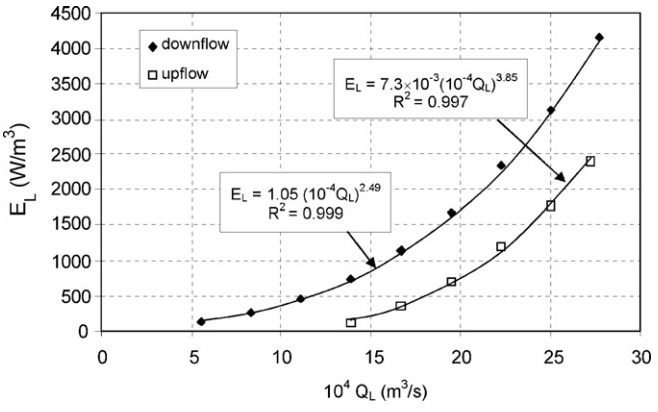

Fig. 4. Evolution of E_L as a function of Q_L.

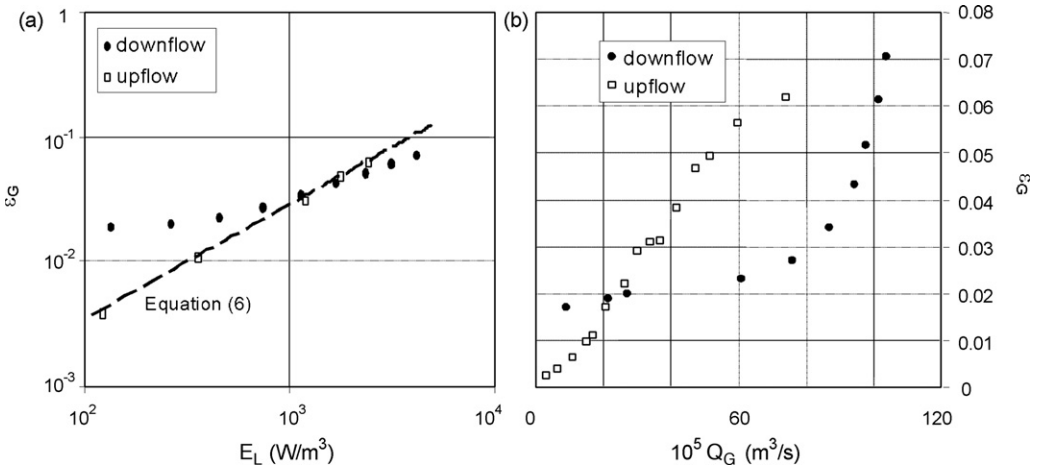

Fig. 5. Evolutions of ε_G as a function of E_L (a) and Q_G (b).

E_L values measured for the upward configuration at constant Q_L stemmed first from the gravitational potential energy term that was never negligible in comparison to the kinetic energy of the liquid phase, even when U_C at the throat was maximum (about 9 m/s in this work). However, this should lead to a nearly constant gap between the two E_L curves at constant Q_L, while Fig. 4 showed that this gap increased with Q_L. As a result, frictional effects due to the differences between the liquid loops in both configurations seemed also to play a role and to be lower for cocurrent upflow. Nevertheless, Q_G remained always higher for cocurrent downflow at constant E_L in this study.

In the downward configuration, two flow regimes had been reported in the *emulsion venturi* [8], depending on the gas–liquid flow ratio:

- the annular flow pattern in which the gas formed a central core with water flowing down through a peripherical annulus along the wall of the divergent at low gas–liquid flow ratio (i.e. the two-phase gas and liquid flow coaxially in the divergent section);
- the homogeneous bubbling regime in which very small bubbles (i.e. the gas–liquid emulsion) occupied all the divergent section at high gas–liquid flow ratio.

This transition was characterized by a maximum in the Q_G/Q_L vs. Q_L plot observed for Q_G/Q_L about 0.59, which corresponded to $Q_{Gm} = 7.9 \times 10^{-4}$ m^3/s (Fig. 2). Similarly, it corresponded to a sudden change of slope in the log–log plot of Q_G vs. E_L, around 600 W/m^3 (Fig. 3). Conversely, these behaviors were never observed for cocurrent upflow: visually, only the homogeneous bubbling conditions were reported. This was in accordance with Figs. 2 and 3 that exhibited neither maximum nor change of slope. However, the Q_G/Q_L ratio was always an increasing function of Q_L in the upward configuration, which differed widely from the behavior observed for the downward configuration in the same flow pattern. These differences resulted mainly from the buoyancy forces that opposed to gas dispersion and favored the formation of a gas core in the divergent in the downward configuration, while they enhanced gas dispersion for cocurrent upflow. Fig. 3 highlights the strong

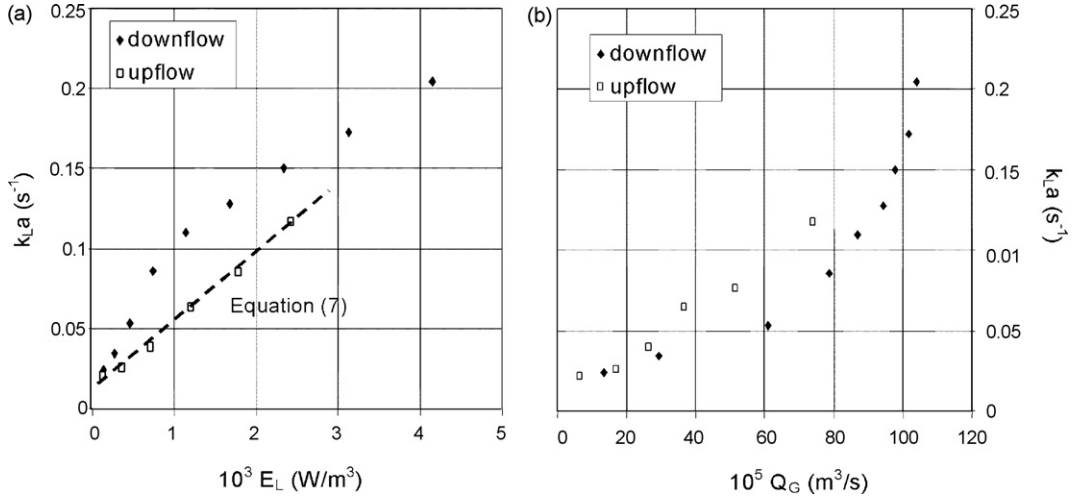

Fig. 6. Evolutions of k_La as a function of E_L (a) and Q_G (b).

influence of flow regime on gas-induced flow rate. Q_G rose steeply in the annular regime, while it increased only slightly in the homogenous flow pattern for cocurrent downflow. Gourich et al. [8] had shown that Q_G varied successively as Q_L^2 and $Q_L^{0.5}$ when Q_L was increased. Conversely, Q_G exhibited a monotonous increase in Fig. 2 in cocurrent upflow and was proportional to Q_L^3, but the correlation coefficient of this expression was poor ($R^2 = 0.95$). A better agreement was obtained when the evolution of Q_G was expressed as a function of E_L:

$$Q_G = 0.161\, E_L^{0.78}\ (R^2 = 0.994) \tag{5}$$

As a comparison, Q_G varied roughly as $E_L^{1.05}$ ($R^2 = 0.98$) in the annular regime and $E_L^{0.16}$ in the homogeneous flow pattern ($R^2 = 0.97$) for cocurrent downflow. This gave an estimation of the crossover point between the two Q_G curves for $E_L \approx 4000\ \mathrm{W/m^3}$ and $Q_G \approx 11 \times 10^{-4}\ \mathrm{m^3/s}$. As a result, the downward configuration could become rather expensive from an energetic point of view if the desired gas flow rate was far higher than Q_{Gm}; cocurrent upflow should therefore be preferred in this case.

The evolution of gas hold-up in the reactor is reported in Fig. 5. This shows that ε_G became higher for cocurrent upflow only when E_L was higher than $1600\ \mathrm{W/m^3}$. As mentioned previously for Q_G, ε_G was adequately correlated to Q_L for cocurrent downflow using power-law models by Gourich et al. [8], but a relationship between ε_G and E_L provided more accurate results for cocurrent upflow (Fig. 5a). In this case, ε_G could therefore be modeled using the following correlation:

$$\varepsilon_G = 4.51 \times 10^{-5}\, E_L^{0.929}\ (R^2 = 0.999) \tag{6}$$

An interesting point is that plotting ε_G vs. Q_L (which can be obtained by combining Figs. 4 and 5) would demonstrate that the downward configuration provides always the highest ε_G values at constant Q_L. This confirms that cocurrent downflow enhanced gas dispersion at fixed Q_L, mainly because gas-induced flow rate was higher (Fig. 2). Conversely, the ε_G vs. Q_G plot showed the opposite behavior for Q_G values between 2×10^{-4} and $7.9 \times 10^{-4}\ \mathrm{m^3/s}$ (Fig. 5b). This was not expected because constant Q_G means higher Q_L for the upward configuration, which gives a lower Q_G/Q_L ratio. Consequently, the ε_G vs. Q_G plot can only be explained by the increase of kinetic energy with Q_L^2 that promotes the formation of smaller bubbles and by the fact that bubble coalescence is reduced when Q_G is lower. These effects compensate apparently the negative impact expected for Q_L increase at constant Q_G on ε_G.

As a conclusion, the Emulsair reactor with cocurrent downflow provided both higher Q_G and ε_G values when Q_L was kept constant. The respective performances of both configurations were closer when E_L was kept constant. On the contrary, the upward configuration provided better results at high-energy input when large Q_G values were desired because it was not sensitive to the flow regime transition observed in cocurrent downflow. Indeed, Q_G seemed to be limited at about $11 \times 10^{-4}\ \mathrm{m^3/s}$ in this configuration, as illustrated by Fig. 5b.

3.2. Mass transfer

Experiments showed that k_La increased continuously when E_L was increased, regardless of reactor configuration (Fig. 6a). In the downward configuration, the influence of flow transition was observed and corresponded to a sudden break of the k_La slope in the k_La vs. E_L curve. Although small bubbles were formed in the homogeneous bubbling regime, the increase of k_La with E_L was slower than in the annular regime, probably because the slope of the Q_G vs. Q_L curve was lower in the homogeneous flow pattern (Fig. 2). Such behavior was not observed in the upward configuration, as expected. Fig. 6a shows clearly that k_La was always higher for the downward than for the upward configuration at constant E_L. However, the increase of k_La vs. E_L was steep both in the annular regime for the downward configuration ($k_La \sim E_L^{0.74}$) and for the upward configuration ($k_La \sim E_L^{0.77}$), but less rapid in the homogeneous regime of the downward configuration ($k_La \sim E_L^{0.48}$). As a result, a crossover point between the two k_La curves could be expected for $E_L \approx 4\ \mathrm{kW/m^3}$, which corresponds roughly to the crossover point expected for Q_G curves in Fig. 3. While k_La was adequately correlated to Q_L in the downward configuration [8], a better agreement was obtained with E_L for cocurrent upflow, in accordance with previous results:

$$k_La = 2.65 \times 10^{-4}\, E_L^{0.77}\ (R^2 = 0.982) \tag{7}$$

This relationship applied in the whole range of E_L values, as no regime transition was observed for this configuration. As already mentioned for ε_G, the gap between the two k_La curves would be amplified in a k_La vs. Q_L plot, but the k_La vs. Q_G plot shows that the upward configuration was more efficient per $\mathrm{m^3}$ gas sucked at the venturi throat (Fig. 6b). This confirms the key role of the kinetic energy of the liquid phase on gas dispersion.

Contrary to previous works [8,9], a and k_L values were measured and they are reported in Figs. 7 and 8 respectively, which allows a better understanding of k_La evolution. The evolution of a in Fig. 7a showed that a values were lower, but only slightly in cocurrent upflow at constant E_L, although Q_G and ε_G were lower in this configuration (Figs. 3 and 5). As a result, a was higher at constant Q_G for cocurrent upflow (Fig. 7b). This behavior could be expected on the basis of the above-mentioned results on ε_G: indeed, the higher kinetic energy of the liquid phase transmitted to the gas in the upward configuration should enhance bubble break-up and reduce coalescence rate, both when either Q_L or E_L were kept constant between both systems (Figs. 2 and 4). It was however not possible in this work to confirm experimentally that bubble diameters were smaller at constant Q_G for the upward configuration. Using the fact that $a = 6\varepsilon_G/d_b$, the average bubble diameters d_b were estimated, but all the values remained around 0.7 ± 0.1 mm and both configurations could not be distinguished, mainly because of the statistical error on ε_G and a measurements. Surprisingly, a did not seem affected by the change in flow regime in the divergent for the downflow configuration. This means that the contribution of the gas core in the annular regime on the interfacial area was negligible, which could however be expected. Thus, the differences in k_La values

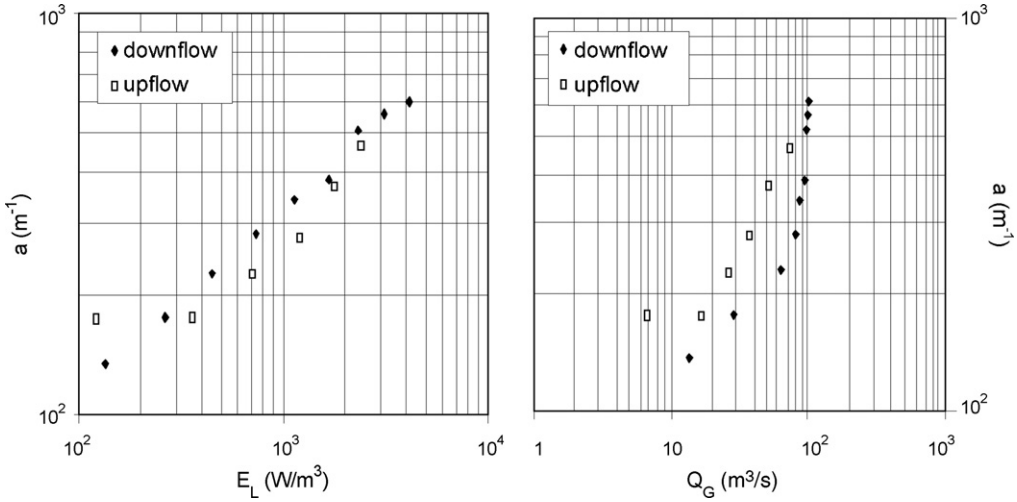

Fig. 7. Evolutions of a as a function of E_L (a) and Q_G (b).

should mainly result from k_L. This conclusion is confirmed by Fig. 8. In the downward configuration, the transition appeared clearly: k_L increased with E_L in the annular regime:

$$k_L = 0.0129\, Q_L^{0.595}\ (R^2 = 0.98) \quad (8)$$

while k_L remained nearly constant in the homogeneous bubbling regime, about 3.8×10^{-4} m/s. This behavior demonstrates surprisingly that k_L depended mainly on Q_G. Indeed, k_L varied steeply when Q_G did the same ($Q_G \sim Q_L^2$), but it became nearly independent of E_L and also Q_L when Q_G varied as $Q_L^{0.5}$. This interpretation is confirmed by Fig. 8b that represents k_L vs. Q_G. As mass transfer takes essentially place in the divergent of the venturi, it seems that Q_G plays a key role in the complex gas–liquid flow rate that occurs in the throat and the divergent and that the relation between k_L cannot be simply related to the turbulent kinetic energy of the liquid phase. This means that bubble-induced turbulence, that depends mainly on Q_G, may prevail, at least when Q_L is high enough. These assumptions are confirmed by the analysis of the results obtained with the upward configuration. First, k_L increased continuously as a function of E_L for cocurrent upflow and followed Eq. (9) as a function of E_L:

$$k_L = 3.26 \times 10^{-5}\, E_L^{2.68}\ (R^2 = 0.99) \quad (9)$$

k_L values were always lower than in the downward configuration at constant E_L (Fig. 8) and the same stood at constant Q_L, as expected. Conversely, they were rather close to those of the downward configuration at constant Q_G, as shown in Fig. 8b, which demonstrates the key importance of Q_G on k_L.

As a conclusion, k_La, k_L and a increased with E_L, Q_L and Q_G in both configurations, despite the flow transition observed in cocurrent upflow. While a values were close at constant specific energy input, which highlights the key role of kinetic energy of the liquid phase on bubble size, k_L values depended mainly on Q_G. As a result, k_La was higher in the downward configuration both at constant Q_L and E_L values, but the opposite behavior was observed at constant Q_G. This shows clearly that the choice between downflow and upflow depends widely on the objec-

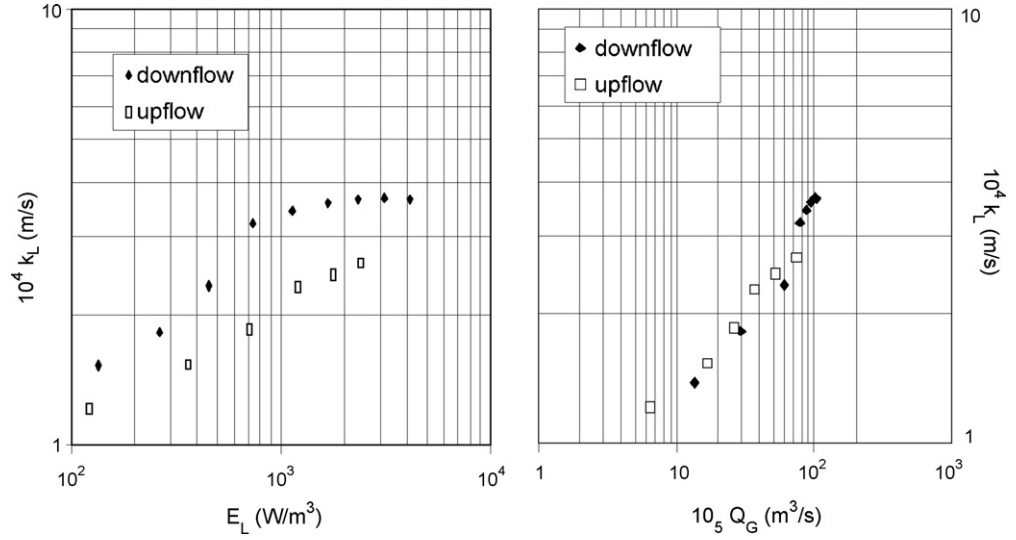

Fig. 8. Evolutions of k_L as a function of E_L (a) and Q_G (b).

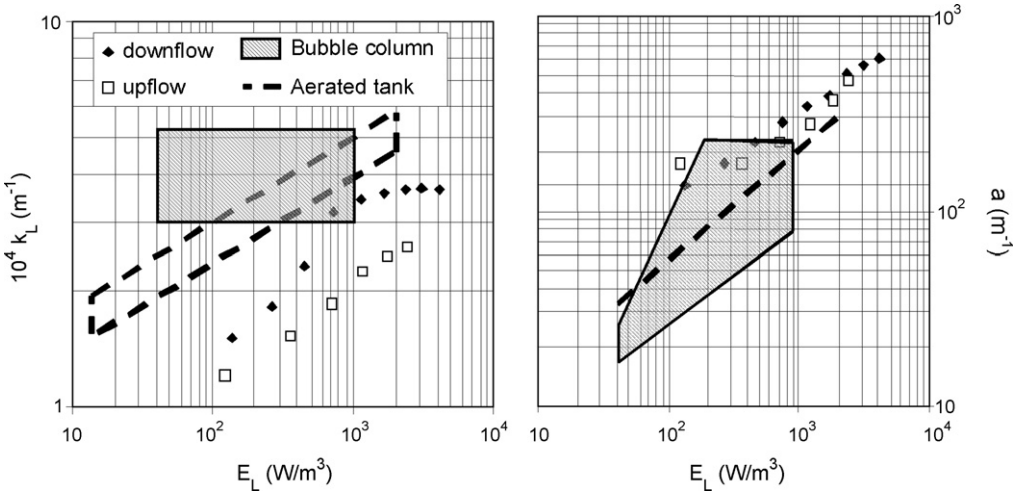

Fig. 9. Comparison of k_L and a values with those of other contacting devices.

tives that have to be achieved: cocurrent upflow can be preferred when high power input or gas flow rates are required because it is not sensitive to the bubbling regime transition, i.e. when they are higher than 4 kW/m^3 and 11×10^{-4} m^3/s in this work, respectively.

3.3. Comparison with other gas–liquid contacting devices

A comparison between bubble columns, airlift reactors, aerated stirred tanks with gas-induction and the cocurrent downflow Emulsair reactor in terms of ε_G, k_La and k_La/ε_G has already been published by Gourich et al. [9]. Figs. 5 and 7 finalize this comparison for the cocurrent upward configuration. The Emulsair reactor presents always the lowest ε_G and k_La values as a function of E_L, regardless of configuration. However, k_La/ε_G was maximum for $E_L > 1$ kW/m^3, which denoted good mass transfer performance per volume of gas when gas–liquid mass transfer became the limiting step. In this region, k_La/ε_G values were between 2 and 3 for the downward configuration, but only between 1 and 2 for cocurrent upflow. For k_L and a, a quantitative comparison with bubble columns equipped with several types of spargers (perforated plate, porous plate, membrane...) and aerated stirred tanks equipped with several types of impellers is presented in Fig. 9. This comparison is supported by literature data on bubble column reactors [2,17–19]. The results for airlift reactors from [20–23] have not been directly reported in Fig. 9 because they correspond to the top right of the region of bubble columns [24]. For stirred reactors with gas-induction, Fig. 9 has also been established both using general data on aerated stirred tanks [2,25–27], but also with specific results on gas-induced devices [28].

As expected, Fig. 9 shows that the Emulsair reactor provides the higher interfacial area, but lower k_L values than bubbles columns and aerated stirred tanks because of the low ε_G (i.e. pneumatically-induced mixing is low) and the lack of mechanical agitation in the reactor respectively. It remains therefore a very versatile tool when the presence of mechanically moving parts has to be avoided and when high and quickly adaptable dissolved gas supply is required as the only operating parameter is the liquid flow rate when the geometry is fixed. This is particularly suitable for fast chemical reactions, but also for biochemical reactions that require high oxygen throughputs during micro-organism growth and for which high oxygen throughputs are not necessary or even unfavorable in the other phases. Similarly, for shear-sensitive micro-organisms, the downflow configuration constitutes an alternative to stirred tanks and airlift reactors, especially when low cost bubble columns are not suitable. This configuration can also be used in the presence of a solid phase and demonstrates therefore a larger applicability than the upward configuration. Additionally to Fig. 9, it has already been shown that the Emulsair reactor presents similar performances as other loop-venturi reactors or ejector-loop reactors [8], but also as reciprocating plate columns [29,30] that do not usually present the same flexibility as the Emulsair reactor. Conversely, the performance of the Emulsair reactor is probably lower than centrifugal field reactors [24], such as rotating packed beds [31], but power requirements are far lower for the Emulsair reactor than for reactors in which gravity is replaced by centrifugal force.

Although this comparison between gas–liquid contacting devices is all but complete because gas dispersion in liquids is still an evolving field, especially with upflow monolith reactors with more and more efficient packings [32], it confirms that the Emulsair reactor (especially the downward configuration), constitutes a versatile gas-inducing device for carrying out complex gas–liquid reactions, for example in the fields of biochemical engineering and environmental engineering, when the gas flow rate must be adapted to requirements that may evolve with time.

4. Conclusions

In this work, a quantitative comparison of hydrodynamic parameters and mass transfer properties of an emulsion-venturi reactor, the Emulsair, has been described between a cocurrent upflow and a cocurrent downflow configuration, both behaving as a gas-inducing device. Quantitative correlations have been

derived, especially for the upward configuration that had not been studied previously. Gas flow rate and specific power input were always lower for cocurrent upflow; the same stood for gas hold-up. Conversely, specific power requirements were lower at constant liquid flow rate and mass transfer properties were enhanced at constant gas-induced flow rate for cocurrent upflow. A comparison with other gas–liquid contacting devices showed that the Emulsair reactor is a versatile tool avoiding the presence of mechanically moving parts when high and quickly adaptable dissolved gas supply is required because it generates high interfacial area at the expense of lower k_L values. The cocurrent upflow configuration can be preferred when high gas flow rates are desired because the evolutions of gas-induced flow rate and mass transfer properties exhibit a stronger dependence on specific power input in the homogeneous bubbling regime for this configuration.

References

[1] J. Villermaux, Génie de la réaction chimique, second ed., Technique et Documentation, Lavoisier, Paris, France, 1993.

[2] M. Bouaifi, G. Hébrard, D. Bastoul, M. Roustan, A comparative study of gas hold-up, bubble size, interfacial area and mass transfer coefficients in stirred gas–liquid reactors and bubble columns, Chem. Eng. Process. 40 (2001), pp. 971–111.

[3] L.X. Huynh, C.L. Briens, J.F. Large, A. Cartros, J.R. Bernard, M.A. Bergougnou, Hydrodynamics and gas–liquid mass transfer in an upward venturi/bubble column combination, Can. J. Chem. Eng. 69 (1991) 711–722.

[4] C.L. Briens, L.X. Huynh, J.F. Large, A. Catros, J.R. Bernard, M.A. Bergougnou, Hydrodynamics and gas–liquid mass transfer in a downward venturi-bubble column combination, Chem. Eng. Sci. 47 (1992) 3549–3556.

[5] P.H.M.R. Cramers, A.A.C.M. Beenackers, L.L. van Dierendonck, Hydrodynamics and mass transfer characteristics of a loop-venturi reactor with a downflow liquid jet ejector, Chem. Eng. Sci. 47 (1992) 3557–3564.

[6] P.H.M.R. Cramers, A.A.C.M. Beenackers, Influence of the ejector configuration, scale and the gas density on the mass transfer characteristics of gas–liquid ejectors, Chem. Eng. J. 82 (2001) 131–141.

[7] P.H.M.R. Cramers, L. Smit, G.M. Leuteritz, L.L. van Dierendonck, A.A.C.M. Beenackers, Hydrodynamics and local mass transfer characteristics of gas–liquid ejectors, Chem. Eng. J. 53 (1993) 67–73.

[8] B. Gourich, M. Belhaj Soulami, A. Zoulalian, M. Ziyad, Simultaneous measurement of gas hold-up and mass transfer coefficient by tracer dynamic technique in "Emulsair" reactor with an emulsion-venturi distributor, Chem. Eng. Sci. 60 (2005) 6414–6421.

[9] B. Gourich, N. El Azher, C. Vial, M. Belhaj Soulami, M. Ziyad, A. Zoulalian, Influence of operating conditions and design parameters on hydrodynamics and mass transfer in an emulsion loop-venturi reactor, Chem. Eng. Process. 46 (2007) 139–149.

[10] K. Tojo, K. Miyanami, Oxygen transfer in jet mixers, Chem. Eng. J. 24 (1982) 89–97.

[11] N.N. Dutta, R.V. Raghavan, Mass transfer and hydrodynamic characteristics of loop reactors Downflow liquidjet ejector, Chem. Eng. Sci. 36 (1987) 111–121.

[12] K. Tahraoui, D. Ronze, A. Zoulalian, Hydrodynamique et transfert gaz-liquide dans un réacteur Verlifix rempli de différents garnissages, Can. J. Chem. Eng. (1992) 636–644.

[13] K. Kiared, A. Zoulalian, Study and modelling of catalytic sulfur dioxide oxidation in "verlifix" three phase reactor, Chem. Eng. Sci. 47 (1992) 3705–3712.

[14] G.B. Liu, K.T. Yu, X.G. Yuan, C.J. Liu, Q.C. Guo, Simulations of chemical absorption in pilot-scale and industrial-scale packed columns by computational mass transfer, Chem. Eng. Sci. 61 (2006) 6511–6529.

[15] C. Alvarez-Fuster, N. Midoux, A. Laurent, J.C. Charpentier, Chemical kinetics of the reaction of carbon dioxide with amines in pseudo m–nth order conditions in aqueous and organic solutions, Chem. Eng. Sci. 35 (1980) 1717–1723.

[16] M. Bouhelassa, A. Zoulalian, Hydrodynamique et transfert gaz liquide dans un bioréacteur du type "Emulsair" fonctionnant en autoaspiration, Entropie 188–189 (1995) 39–45.

[17] Y.T. Shah, B.G. Kelkar, S.P. Godbole, W.-D. Deckwer, Design parameters estimations for bubble column reactor, AIChE J. 28 (1982) 353–379.

[18] W.-D. Deckwer, Bubble Column Reactors, J. Wiley & Sons, Chichester, UK, 1992.

[19] J. Zahradník, M. Fialová, M. Růžička, J. Drahoš, F. Kaštánek, N.H. Thomas, Duality of the gas–liquid flow regimes in bubble column reactors, Chem. Eng. Sci. 52 (1997) 3811–3826.

[20] Y. Chisti, M. Moo-Young, Airlift reactors: characteristics, applications and design considerations, Chem. Eng. Commun. 60 (1987) 195–242.

[21] Y. Chisti, Airlift Bioreactors, Elsevier, New York, USA, 1989.

[22] J.C. Merchuk, M. Gluz, Airlift bioreactors, in: M.C. Flickinger, S.W. Drew (Eds.), Encyclopedia of Bioprocess Technology, 1, John Wiley & Sons, New York, 1999, pp. 320–353.

[23] J.B. Joshi, V.V. Ranade, S.D. Gharat, S.S. Lele, Sparged loop reactors, Can. J. Chem. Eng. 68 (1990) 705–741.

[24] A. Mersmann, G. Schneider, H. Voit, E. Wenzig, Selection and design of aerobic bioreactors, Chem. Eng. Technol. 13 (1990) 357–370.

[25] S. Nagata, Mixing, Principles and Application, Kodansha Ltd., Japan, 1975.

[26] N. Harnby, M.F. Edwards, A.W. Nienow, Mixing in Process Industries, Butterworths-Heinemann, Oxford, UK, 1992.

[27] C. Xuereb, M. Poux, J. Bertrand, Agitation et mélange – Aspects fondamentaux et applications industrielles, Dunod, Paris, France, 2006.

[28] S. Poncin, C. Nguyen, N. Midoux, J. Breysse, Hydrodynamics and volumetric gas–liquid mass transfer coefficient of a stirred vessel equipped with a gas-inducing impeller, Chem. Eng. Sci. 57 (2002) 3299–3306.

[29] M.R. Hewgill, M.R. Mackley, A.B. Pandit, S.S. Pannu, Enhancement of gas–liquid mass transfer using oscillatory flow in baffled tubes, Chem. Eng. Sci. 48 (1993) 799–809.

[30] M.H.I. Baird, N.V. Rama Rao, P. Stonestreet, Power dissipation and hold-up in a gassed reciprocating baffle plate column, Trans. IchemE. 74A (1996) 463–469.

[31] Y.S. Chen, C.-C. Lin, H.S. Liu, Mass transfer in a rotating packed bed with various radii of the bed, Ind. Eng. Chem. Res. 44 (1990) 7868–7875.

[32] C.O. Vandu, J. Ellenberger, R. Krishna, Hydrodynamics and mass transfer in an upflow monolith loop reactor, Chem. Eng. Process. 44 (2005) 363–374.